Biophysical Journal Volume 68 March 1995 1128–1136

# 2D Exchange $^{31}$P NMR Spectroscopy of Bacteriophage M13 and Tobacco Mosaic Virus

Pieter C. M. M. Magusin and Marcus A. Hemminga
Department of Molecular Physics, Wageningen Agricultural University, 6703 HA Wageningen, The Netherlands

ABSTRACT Two-dimensional (2D) exchange $^{31}$P nuclear magnetic resonance spectroscopy is used to study the slow overall motion of the rod-shaped viruses M13 and tobacco mosaic virus in concentrated gels. Even for short mixing times, observed diagonal spectra differ remarkably from projection spectra and one-dimensional spectra. Our model readily explains this to be a consequence of the $T_{2e}$ anisotropy caused by slow overall rotation of the viruses about their length axis. 2D exchange spectra recorded for 30% (w/w) tobacco mosaic virus with mixing times <1 s do not show any off-diagonal broadening, indicating that its overall motion occurs in the sub-Hz frequency range. In contrast, the exchange spectra obtained for 30% M13 show significant off-diagonal intensity for mixing times of 0.01 s and higher. A log-gaussian distribution around 25 Hz of overall diffusion coefficients mainly spread between 1 and $10^3$ Hz faithfully reproduces the 2D exchange spectra of 30% M13 recorded at various mixing times in a consistent way. A small but notable change in diagonal spectra at increasing mixing time is not well accounted for by our model and is probably caused by $^{31}$P spin diffusion.

## INTRODUCTION

In the past few years, two-dimensional (2D) exchange nuclear magnetic resonance (NMR) spectroscopy has proven its value for studying motion in a broad range of systems such as synthetic polymers (Schmidt-Rohr and Spiess, 1991), lipids (Fenske and Jarrell, 1991), liquids (Kimich and Fischer, 1994), and liquid-gas interfaces (Tomasselli et al., 1993). Some processes, such as exchange of nuclear spins between different chemical or physical environments, translation of spins in a field gradient, or reorientation of nuclei with chemical shift anisotropy (CSA) with respect to the magnetic field, can correlate different resonance positions in the NMR spectrum through time. By the use of 2D exchange NMR spectroscopy, this correlation can be made visible as a cross-peak, or, more general by, off-diagonal intensity in 2D NMR spectra, which are therefore easy to interpret, at least in a qualitative manner. Quantitatively, 2D exchange spectra dominated by specific reorientational processes have been analyzed in terms of combined subspectra representing different reorientation angles (Wefing et al., 1988). The possibility to extract the distribution of reorientation angles directly from the spectrum is especially useful for studying amorphous materials containing internal motions without sharply defined restriction angles and correlation times.

In previous work, we have presented analyses of one-dimensional (1D) $^{31}$P NMR spectra and transversal relaxation decays of bacteriophage M13 and tobacco mosaic virus (TMV) (Magusin and Hemminga, 1993b, 1994). M13 and TMV are rod-shaped viruses with a length of ~900 and 300 nm and a diameter of ~9 and 18 nm, respectively. Intact virus particles largely consist of a protein coat protecting the encapsulated viral genome, which contributes only a small part of the particle weight. Because the coat proteins of M13 and TMV do not contain $^{31}$P nuclei, selective information about the structure and dynamics of the phosphodiesters in the encapsulated nucleic acid molecule can be obtained by the use of $^{31}$P NMR spectroscopy. The way in which $^{31}$P NMR powder lineshapes and transversal relaxation observed for M13 and TMV are influenced by motion cannot be explained consistently by simple models such as, e.g., isotropic rotational diffusion or rotation of the rod-shaped virions about their length axis alone (Magusin and Hemminga, 1993b). Instead, a combination of fast, restricted nucleic acid backbone motion and slow overall motion of the virions is found. Fast, restricted backbone motion also explains the fact that sideband intensities in magic angle spinning (MAS) spectra of dilute M13 gels (Magusin and Hemminga, 1994) deviate from the values predicted by standard theory (Herzfeld and Berger, 1980). The spinning-rate dependence of MAS transversal relaxation has successfully been assigned to slow overall rotation of the virions as a whole (Magusin and Hemminga, 1994). To test and refine this model further, we have investigated the slow overall motion of the rod-shaped viruses in concentrated gels using 2D exchange $^{31}$P NMR spectroscopy. The results of this investigation are presented and analyzed in this paper.

## THEORY

To calculate the effect of rotational diffusion of the rod-shaped virions about their length axis on $^{31}$P 2D exchange spectra, the orientation of a $^{31}$P chemical shift tensor is first expressed by use of the Euler angles $\Omega = (\alpha, \beta, \gamma)$ in an axis system fixed to the virion with its $z$ axis parallel to the length axis of the virion. The orientation of this rotor axis system in the laboratory frame with the $z$ axis parallel to the magnetic field, in turn, is given by $\Omega' = (\phi, \theta, \psi)$. If interactions between $^{31}$P and other nuclei are negligible, transversal and longitudinal $^{31}$P magnetization can be calculated from the positive- and negative-helicity components $\mu_{\pm}(\Omega, \Omega', t)\mathbf{I}_{\pm}$ of the spin density operator $\rho(\Omega, \Omega', t)$ and its longitudinal component $\mu_z(\Omega, \Omega', t)\mathbf{I}_z$. In the presence

*Received for publication 12 October 1994 and in final form 21 December 1994.*

Address reprint requests to Dr. Marcus A. Hemminga, P. O. Box 8128, 6700 ET Wageningen, The Netherlands. Tel.: 31-8370-82635/82044; Fax: 31-8370-82725; E-mail: marcus.hemminga@virus.mf.wau.nl.



0006-3495/95/03/1128/09 $2.00

of only Zeeman interaction, chemical shift, and rotational diffusion, the relevant equations for these three components derived from the stochastic Liouville equation are represented in the rotating frame by

$$\frac{d\mu_{\pm}(\Omega, \Omega', t)}{dt} = \left(\pm i\omega(\Omega, \Omega') + D\frac{\partial^2}{\partial\psi^2}\right)\mu_{\pm}(\Omega, \Omega', t) \qquad (1a)$$

and

$$\frac{d\mu_z(\Omega, \Omega', t)}{dt} = D\frac{\partial^2}{\partial\psi^2}\mu_z(\Omega, \Omega', t) \qquad (1b)$$

where $D$ denotes the diffusion coefficient for the overall virion motion and $\omega(\Omega, \Omega')$ represents the chemical shift interaction, expressed in terms of the Wigner functions $D^2_{m'm}(\alpha\beta\gamma) = \exp(im'\gamma)d^2_{m'm}(\beta)\exp(im\alpha)$ (Edmonds, 1960; Haeberlen, 1976) as

$$\omega(\Omega, \Omega') = \omega_o\sigma_o + \omega_o\sum_{m'=-2}^{2} D^2_{m'0}(\Omega')[F_0D^2_{0m'}(\Omega) + F_2(D^2_{2m'}(\Omega) + D^2_{-2m'}(\Omega))] \qquad (2a)$$

where $\omega_o = \gamma B_o$ is the Zeeman angular frequency, $\sigma_o = (\sigma_{11} + \sigma_{22} + \sigma_{33})/3$, $F_0 = (\sigma_{33} - \sigma_o)$ and $F_2 = (\sigma_{11} - \sigma_{22})/\sqrt{6}$ for a chemical shift tensor with tensor values $\sigma_{11}$, $\sigma_{22}$, and $\sigma_{33}$. In our previous analyses of $^{31}$P powder lineshapes and MAS spectra of M13 and TMV, we have described the net effect of fast, restricted backbone motions of the encapsulated nucleic acid molecule in a simplified way, as the effect caused by fast, restricted diffusion of the phosphodiesters about the length axis of the virions. Also here we will assume that the phosphodiesters undergo uniaxial diffusion restricted to angles $\alpha \in [\alpha_o - \lambda, \alpha_o + \lambda]$, fast enough to allow us to replace $D^2_{nm'}(\Omega)$ $(n = 0, \pm 2)$ in Eq. 2a by the average value $D^2_{nm'}(\Omega_o)\,\mathrm{sinc}(m'\lambda)$, where $\Omega_o = (\alpha_o, \beta, \gamma)$ and $\mathrm{sinc}(m'\lambda)$ denotes the function $\sin(m'\lambda)/m'\lambda$, which yields

$$\omega_\lambda(\Omega_o, \Omega') = \omega_o\sigma_o + \omega_o\sum_{m'=-2}^{2} d^2_{m'0}(\theta)[F_0d^2_{0m'}(\beta) + F_2(d^2_{2m'}(\beta)e^{2i\gamma} + d^2_{-2m'}(\beta)e^{-2i\gamma})]\,e^{im'(\psi+\omega_o)}\mathrm{sinc}(m'\lambda) \qquad (2b)$$

The development of transversal coherence $\mu_{\pm}(\Omega, \Omega', t)$ would follow from the solution of Eq. 1a. Unfortunately, this equation cannot be solved analytically. For very slow rotational diffusion with a coefficient $D$ much smaller than the static linewidth of about $\omega_o|\sigma_{33} - \sigma_{11}|$, however, spin density may be assumed to stay close to its initial orientation within times in the order of the decay time of the free induction decay and it is then justified to linearize Eq. 1a by approximating $\omega_\lambda(\Omega_o, \Omega')$ for orientations closely around any orientation $\Omega'_o = (\phi, \theta, \psi_o)$ as $\omega_\lambda(\Omega_o, \Omega'_o) + g_\lambda(\Omega_o, \Omega'_o)(\psi - \psi_o)$, where $g_\lambda(\Omega_o, \Omega'_o)$ denotes the derivative $\partial\omega_\lambda/\partial\psi$ for $\psi = \psi_o$. The linearized Eq. 1a may be solved in a manner similar to the case of spins diffusing in a linear field gradient (Slichter, 1978), from which the two transversal components of spin density at orientations infinitely close to $\Omega'_o$ may be derived as

$$\mu_{\pm}(\Omega_o, \Omega'_o, t) = \exp[-Dr_\lambda(\Omega_o, \Omega'_o)\,t^3 \pm i\omega_\lambda(\Omega_o, \Omega'_o)t]\mu_{\pm}(\Omega_o, \Omega'_o, 0) \qquad (3a)$$

where

$$r_\lambda(\Omega_o, \Omega'_o) = [g_\lambda(\Omega_o, \Omega'_o)]^2/3 \qquad (3b)$$

Analogously, a $\pi$ pulse at time $\tau$ after the excitation pulse produces an echo at time $2\tau$ given by

$$E_{\pm}(\Omega_o, \Omega'_o, 2\tau) = \exp[-Dr_\lambda(\Omega_o, \Omega'_o)2\tau^3]\mu_{\pm}(\Omega_o, \Omega'_o, 0) \qquad (4)$$

Eq. 4 shows that in a first approximation very slow overall diffusion causes a type of transversal relaxation that is non-exponential, non-fluctuating and anisotropic. An apparent relaxation time $T_{2e}$ may be defined as the time $2\tau$ at which the powder echo $\langle E_{\pm}(\Omega_o, \Omega'_o, 2\tau)\rangle$ decays to $e^{-1}$ of its initial value. It follows from Eq. 4 that $T_{2e}$ is inversely proportional to the cube root of $D$.

In the absence of $T_1$ relaxation and spin diffusion, the development of longitudinal coherence $\mu_z(\Omega, \Omega', t)$ is only determined by the overall motion of the rod-shaped virions. Therefore, from a given longitudinal coherence distribution $\mu_z(\Omega, \Omega'_1, t_1)$ at a specific time $t_1$, the coherence distribution $\mu_z(\Omega, \Omega'_2, t_1 + t_m)$ at a later time $t_1 + t_m$ can be calculated by integrating the fraction of coherence associated to each virion orientation $\Omega'_1 = (\phi_1, \theta_1, \psi_1)$ that is transferred to the orientation $\Omega'_2 = (\phi_2, \theta_2, \psi_2)$ between $t_1$ and $t_1 + t_m$

$$\mu_z(\Omega, \Omega'_2, t_1 + t_m) = \int P(\Omega'_2|\Omega'_1, t_m)\mu_z(\Omega, \Omega'_1, t_1)\,d\Omega'_1 \qquad (5)$$

where $P(\Omega'_2|\Omega'_1, t_m)$ may also be regarded as the conditional probability density of finding a virion in orientation $\Omega'_2$ provided that its orientation was $\Omega'_1$ a time $t_m$ before. For uniaxial rotational diffusion of the rod-shaped virions about their length axis, $P(\Omega'_2|\Omega'_1, t_m)$ follows from Eq. 1b as

$$P(\Omega'_2|\Omega'_1, t_m) = \frac{\delta(\varphi_2 - \varphi_1)\,\delta(\theta_2 - \theta_1)}{(4\pi Dt_m)^{1/2}}\sum_{k=-\infty}^{\infty}\exp\left[-\frac{(\psi_2 - \psi_1 - 2k\pi)^2}{4Dt_m}\right] \qquad (6)$$

where $\delta(\phi_2 - \phi_1)$ and $\delta(\theta_2 - \theta_1)$ represent Dirac's $\delta$ functions and the summation over $k$ has been included in the definition of $P(\Omega_2|\Omega_1, t_m)$ to let the integration boundaries in Eq. 3a be standard ones, more specifically $0 < \psi_1 < 2\pi$. If $t_m$ reduces to 0, $P(\Omega'_2|\Omega'_1, t_m)$ becomes the 3D $\delta$ function $\delta(\phi_2 - \phi_1)\,\delta(\theta_2 - \theta_1)\,\delta(\psi_2 - \psi_1)$, as expected.

The pulse sequence employed in our experiments to record 2D exchange NMR spectra is depicted in Fig. 1. Transversal $^{31}$P magnetization is first created from $^1$H magnetization using cross-polarization. During the ensuing evolution time $t_1$ the orientations of the virions are indirectly probed by labeling $^{31}$P magnetization with the anisotropic chemical shift. After $t_1$, the $x$ or $y$ component is rotated along the $z$ direction and during the ensuing mixing time $t_m$, the orientations of the virus particles are allowed to change. To probe the new orientations, the $z$ magnetization of the $^{31}$P magnetization is rotated back to the transversal plane and the echo produced by a $\pi$ pulse at a short time $\Delta$ after back-rotation is measured during the detection time $t_2$. The NMR signal that results from the pulse sequence in Fig. 1 depends on the phase shifts between the pulses. By varying these phase shifts different NMR signals can be generated which in combination produce a purely amplitude modulated signal

$$S(t_1, t_2|t_m) = (8\pi^2)^{-3}\int\int\int d\Omega_o\,d\Omega'_1\,d\Omega'_2P(\Omega'_2|\Omega'_1, t_m) \times \exp[-Dr_\lambda(\Omega_o, \Omega'_1)t_1^3]\cos(\omega_\lambda(\Omega_o, \Omega'_1)t_1) \times \exp[-Dr_\lambda(\Omega_o, \Omega'_2)(2\tau^3 + t_2^3)]\cos(\omega_\lambda(\Omega_o, \Omega'_2)t_2) \qquad (7)$$

as can be derived by use of Eqs. 3a, 3b, 4a, and 4b.

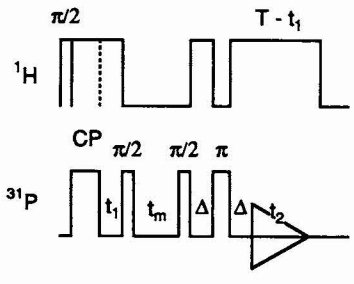


FIGURE 1 Pulse sequence with $^1$H and $^{31}$P pulses (above and below, respectively) used for 2D exchange $^{31}$P NMR spectroscopy. CP denotes the cross-polarization contact time. A $\pi$ pulse creates the echo measured during detection time $t_2$. High-power proton decoupling is on during the evolution time $t_1$, refocusing delays $\Delta$ and detection time $t_2$. By decreasing the length of the final decoupling pulse at increasing $t_1$, proton decoupling is on during a constant time $T$, so that the sample-heating caused by it is kept constant to prevent temperature drift.

In principle, 2D exchange spectra $I(\omega_1, \omega_2 | t_m)$ may be simulated for various diffusion coefficients $D$ by Fourier transformation of the 2D signals $S(t_1, t_2 | t_m)$ generated by use of Eq. 7. The integration over chemical shift tensor orientations $\Omega_o$, virus orientations $\Omega'_1$ and $\Omega'_2$, and diffusion coefficients $D$, however, makes such calculations too lengthy to be of practical use. The calculation time may be strongly reduced by making some approximations. First, lineshape effects caused by transversal relaxation during short echo delays $2\tau$ are only small. This has been experimentally observed for M13 and is also calculated theoretically for uniaxial diffusion of M13 as a whole, if it is assumed that phosphodiesters are randomly oriented within the phage (Magusin and Hemminga, 1993a). The angular-dependent relaxation factor $\exp[-D\, r(\Omega_o, \Omega'_2)2\tau^3]$ in Eq. 7 may then be approximated by an isotropic factor $\exp[-D < r > 2\tau^3]$, which can be drawn outside the angular integrals. This makes Eq. 7 symmetrical with respect to exchange between $t_1$ and $t_2$, so that $S(t_1, t_2 | t_m)$ needs only be calculated for $t_1 \leq t_2$, which halves the calculation time.

A further reduction of calculation time is possible if one single set of subspectra generated only once, can be used in different combinations to simulate 2D exchange spectra for various diffusion coefficients and mixing times. A similar procedure for analyzing 2D exchange spectra in terms of jump angle distributions has been presented elsewhere (Wefing et al., 1988, Wefing and Spiess, 1988). $P(\Omega'_2 | \Omega'_1, t_m)$ (Eqs. 6 and 8) depends on the rotation angle $\Delta\Omega' = \Omega'_2 - \Omega'_1$ rather than on the orientation angles $\Omega'_2$ and $\Omega'_1$ separately. After Fourier transformation, we therefore apply the coordinate transform $(\Omega'_1, \Omega'_2) \rightarrow (\Omega'_1, \Delta\Omega')$ to Eq. 7, substitute $P(\Omega'_1 + \Delta\Omega' | \Omega'_1, t_m)$ by $P(\Delta\Omega' | t_m)$, and finally approximate the integral over $\Delta\Omega'$ by a summation over a set of subspectra $I_n(\omega_1, \omega_2 | \Delta\Omega'_n)$ for a series of equidistant values $\Delta\Omega'_n$ to obtain

$$I(\omega_1, \omega_2 | t_m) = \sum P(\Delta\Omega'_n | t_m) I_n(\omega_1, \omega_2 | \Delta\Omega'_n) \tag{8}$$

Strictly mathematically, subspectra $I_n(\omega_1, \omega_2 | \Delta\Omega'_n)$ still depend on the diffusion coefficient D through transversal relaxation (Eq. 7), so that different sets of subspectra would still have to be calculated to simulate 2D exchange spectra for different diffusion coefficients. For long mixing times however, the effect of transversal relaxation during $t_1$ and $t_2$ on the off-diagonal intensity is generally negligible with respect to the off-diagonal intensity caused by the large orientational changes taking place during $t_m$. As a consequence, subspectra generated for some specific $D$ value can actually well be used to simulate exchange spectra for a complete range of diffusion coefficients. In our calculations we therefore make an artificial distinction between rotational diffusion with diffusion coefficient $D_o$ taking place during $t_1$ and $t_2$, and diffusion with coefficient $D$ during $t_m$. A value for $D_o$ can be independently estimated from transversal $^{31}$P relaxation measurements (Magusin and Hemminga, 1993b), so that only the diffusion coefficient $D$ remains to be determined from 2D exchange NMR spectra. The subspectra are then given by

$$\begin{aligned} I_n(\omega_1, \omega_2 | \Delta\Omega'_n) &= (8\pi^2)^{-2} \exp[-D_o < r > 2\tau^3] \\ &\times \int dt_1 e^{i\omega_1 t_1} \int dt_2\, e^{i\omega_2 t_2} \int\int d\Omega_o\, d\Omega'_1 \\ &\times \exp[-D_o r_\lambda(\Omega_o, \Omega'_1) t_1^3] \cos(\omega_\lambda(\Omega_o, \Omega'_1) t_1) \\ &\times \exp[-D_o r_\lambda(\Omega_o, \Omega'_1 + \Delta\Omega'_n) t_2^3] \cos(\omega_\lambda(\Omega_o, \Omega'_1 + \Delta\Omega'_n) t_2) \end{aligned} \tag{9}$$

Because $P(\Delta\Omega' | t_m)$ does not depend on the sign of the rotation (Eq. 6), the summation in Eq. 8 may be further simplified by combining subspectra for positive and negative $\Delta\Omega'_n$ beforehand, yielding

$$I_n^{\pm}(\omega_1, \omega_2 | \Delta\Omega'_n) = \begin{cases} I_n(\omega_1, \omega_2 | \Delta\Omega'_n) + I_n(\omega_1, \omega_2 | -\Delta\Omega'_n), & \text{if } \Delta\Omega'_n \neq 0 \\ I_n(\omega_1, \omega_2 | 0), & \text{if } \Delta\Omega'_n = 0 \end{cases} \tag{10}$$

In the derivation of Eq. 8 it is assumed that all virions in the gel undergo rotational diffusion with the same diffusion coefficient $D$. However, local viscosity differences in the concentrated gels could exist, causing variations in rotational diffusion. To include the effect of motional inhomogeneity, it is assumed in the model that the logarithmic values $\log(D)$ of the diffusion coefficients $D$ are symmetrically distributed around some central value $\log(D_c)$ according to a Gaussian density function with characteristic width $W$ (Wefing et al., 1988). For simplicity, rotational diffusion during $t_1$ and $t_2$ is considered to be homogeneous and independent of diffusion during $t_m$. For the case of inhomogeneous diffusion, $P(\Delta\Omega'_n | t_m)$ in Eq. 8 must be replaced by

$$\begin{aligned} P'(\Delta\Omega' | t_m) = \frac{\delta(\Delta\varphi)\delta(\Delta\theta)}{2\pi(Wt_m)^{1/2}} \int_{-\infty}^{\infty} \exp\left[-\left\{\frac{\log(D) - \log(D_c)}{W}\right\}^2\right] \\ \times \frac{1}{D^{1/2}} \sum_{k=-\infty}^{\infty} \exp\left[\frac{(\Delta\psi + 2k\pi)^2}{4Dt_m}\right] d\log(D) \end{aligned} \tag{11}$$

where $\Delta\phi = \phi_2 - \phi_1$, $\Delta\theta = \theta_2 - \theta_1$ and $\Delta\psi = \psi_2 - \psi_1$. For $W$ approaching 0, Eq. 8 reduces to Eq. 6 again.

## MATERIALS AND METHODS

### Experimental procedures

M13 and TMV were grown, purified and concentrated to 30% (w/w) as described previously (Magusin and Hemminga, 1993b). NMR spectra were recorded on a Bruker CXP300 spectrometer (Bruker Instruments, Inc., Billerica, MA) operating at a $^{31}$P NMR frequency of 121.5 MHz. 2D exchange $^{31}$P NMR spectra were recorded using the pulse sequence depicted in Fig. 1, which involves cross-polarization to create transversal $^{31}$P magnetization and a Hahn-echo-producing $\pi$ pulse to remove the effect of probe ringing on the weak signal. Because of the dielectric properties of wet M13 and TMV gels, the $\pi/2$ pulse was set to 5 $\mu$s on the weak $^{31}$P NMR signal of the sample itself. The Hartmann-Hahn condition necessary for cross-polarization was found by measuring the $^1$H $\pi/2$ pulse length directly on the water signal and setting it equal to the $^{31}$P $\pi/2$ pulse length. The dwell time was 5 $\mu$s, and the carrier frequency was set to the center of the $^{31}$P resonance. To record spectra of M13, $t_1$ was systematically incremented by 5 $\mu$s. For TMV the $t_1$ increment was 10 $\mu$s. CYCLOPS phase alternation was employed to remove the effects of pulse imperfections and time-proportional phase incrementing was used to acquire the spectra in the phase-sensitive mode (Marion and Wüthrich, 1983). Phase cycling of the first proton pulse suppressed the effect of direct $^{31}$P excitation on the signal. Signals were recorded with 256 data points. To avoid truncation effects and to obtain the best signal-to-noise ratio within the measuring time available, the number of $t_1$ increments ($NE$) and the number of scans per $t_1$ increment ($NS$) were chosen differently for different mixing times $t_m$. M13 spectra for $t_m = 0.1$ and 1.0 s were recorded with $NE = 64$ and $NS = 1024$. For $t_m = 0.01$ s these numbers were both 128. TMV spectra were acquired with $NE = 128$ and $NS = 512$. The repetition time was 1.1 s. Two dummy scans were used to get the spin system in a steady state. High-power proton decoupling was on during cross-polarization (1.0 ms), the variable evolution time $t_1$, refocusing delays $\tau$ and acquisition time $t_{aq}$ (1.4 ms). An extra decoupling delay at the end of the pulse sequence was shortened at increasing $t_1$ so that the total decoupling time per experiment was kept constant at ~3 ms. In this way, the temperature could be kept constant at 30°C throughout the experiment by use of a Bruker temperature unit, as checked using a fluoroptic thermometer as described previously (Magusin and Hemminga, 1993b). Sample tubes were sealed with a two-component glue to keep the water content in the gel constant; this was checked by weighting and spectrophotometry.

### Simulation procedures

2D exchange $^{31}$P NMR spectra at 121.5 MHz were simulated for M13 using Fortran programs derived from the equations in this paper. For the chemical shift tensor of $^{31}$P nuclei in M13 the relative tensor values $\sigma_{11} - \sigma_o = 77$ ppm, $\sigma_{22} - \sigma_o = 18$ ppm, and $\sigma_{33} - \sigma_o = -95$ ppm (where $\sigma_o$ is the isotropic shift) were taken (Magusin and Hemminga, 1993b, 1994). In the simulations it was assumed that a random distribution of shift tensor orientations exists

within M13. To analyze experimental spectra, a set of 16 subspectra was first generated in a numerical way approximating Eq. 9 for a series of jump angles $\Delta\Omega'_n = (0, 0, \Delta\Psi_n)$ with $\Delta\Psi_n$ being multiples of 0.2 rad between 0.0 and 3.0 rad. Next, these subspectra were combined according to Eq. 8 with $P(\Delta\Omega' \mid t_m)$ or $P'(\Delta\Omega' \mid t_m)$ calculated for various mixing times and diffusion coefficients. These linear combinations were fitted to the experimental spectrum allowing height of the simulated spectrum to vary. The best-fitting linear combination was found by comparing the variance between the theoretical spectra and the observed spectrum.

## RESULTS

Fig. 2 shows contour plots of the 2D exchange $^{31}$P NMR spectra of 30% M13 and 30% TMV recorded with a mixing time $t_m = 1$ s. To facilitate comparison between the two, the contour in the TMV spectrum has been drawn at the same relative intensity level, 23%, as the middle contour in the M13 spectrum. For TMV, this contour lies practically on the diagonal, indicating that most phosphodiesters in TMV do not undergo large reorientations at the time scale of seconds. In contrast, the 23% contour in the spectrum of M13 illustrates a large spread of spectral intensity in the frequency plane. The approximately hexagonal shape of the 10% contour reflects the three discontinuities in the 1D $^{31}$P powder lineshape. At shorter mixing times, these discontinuity features of the 10% contour become less prominent. Narrower, elliptically shaped contours are observed in spectra recorded with $t_m = 0.1$ s. The width of this ellipse further reduces as $t_m$ decreases to 0.01 s, and for $t_m \leq 0.001$ s, only a narrow diagonal ridge is visible in 2D exchange NMR spectra of 30% M13.

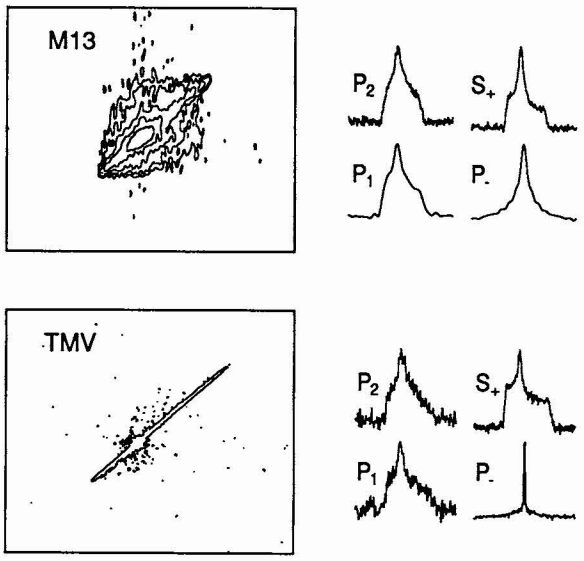


FIGURE 2 2D exchange spectra of 30% M13 and TMV for $t_m = 1$ s. The contours shown for M13 represent levels of 10, 15, 23, 33, and 50% with respect to the highest intensity at the $\sigma_{22}$ position on the diagonal. Only the 23% contour is shown for TMV. $P_2$ and $P_1$ are the spectral projections on the $\nu_2$ and $\nu_1$ axis, respectively, $S_+$ denotes the spectral cross-section along the diagonal and $P_-$ is the projection on the antidiagonal. Frequency ranges shown are 50 kHz for $P_2$ and $P_1$, $50 \times \sqrt{2}$ kHz for $S_+$ and $50/\sqrt{2}$ kHz for $P_-$. No filtering or symmetrization has been used to create the figure. The $w_1$- and $w_2$-axes are in vertical and horizontal direction, respectively.

Theoretical studies have pointed out that homogeneous jumplike motions would often cause characteristic ridge patterns to show up in 2D exchange spectra (Wefing and Spiess, 1988; Wefing et al., 1988). No such ridge patterns are present in 2D exchange spectra of M13. Instead, intensity curves in spectral cross-sections taken at right angles with respect to the spectrum diagonal, generally have gaussian shapes, gradually broadening at increasing $t_m$. Such a type of antidiagonal broadening is indicative of rotational diffusion dominating 2D exchange (Wefing et al., 1988). Interestingly, 2D exchange spectra of 15% M13 recorded with mixing times of 0.001 and 0.01 s (not shown) are very similar to the 30% M13 spectra recorded with mixing times of 0.01 and 0.1 s, respectively (Fig. 3). This directly indicates that, if one type of motion mainly underlies the observed off-diagonal broadening at both concentrations, this motion should be about 10 times faster in 15% than in 30% M13 gels. This, in turn, would agree with the factor 8 difference between the diffusion coefficients, which we estimated previously by interpreting transversal relaxation in terms of slow overall rotation of the rod-shaped M13 virions about their length axis (Magusin and Hemminga, 1993b).

Remarkably, the diagonal cross-section $S_+$ in 2D exchange spectra of M13 and TMV recorded even at vanishing mixing times (10 $\mu$s) strongly differs from the corresponding 1D $^{31}$P NMR spectra. Discontinuities are generally more pronounced in $S_+$ than in the projection $P_2$ on the $\nu_2$ axis, which represents the Fourier transform of the time-domain cross-section $S(0, t_2 \mid t_m)$. In the absence of $T_1$ anisotropy, $P_2$ should be similar to the 1D spectrum. This phenomenon cannot be explained by the experimental asymmetry of the $t_1$ and $t_2$ time domains with regard to the Hahn-echo pulse-sequence preceding $t_2$, but not $t_1$ (Fig. 1). The absence of a true $t_1 = 0$ measurement would distort the projection $P_1$ on the $\nu_1$ axis more than the lineshape in the diagonal spectrum $S_+$, which

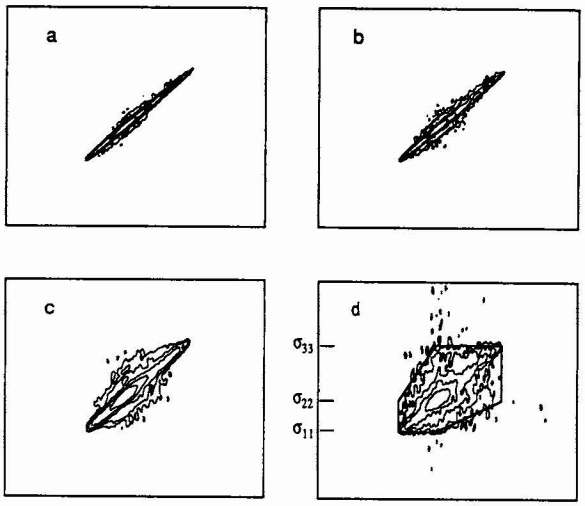


FIGURE 3 Contour plots of 30% M13 spectra recorded for $t_m = 0.001$ (*a*), 0.01 (*b*), 0.1 (*c*), and 1 s (*d*), respectively. Contour levels are the same as in Fig. 2. The hexagon reflecting the chemical shift tensor values $\sigma_{11}$, $\sigma_{22}$, and $\sigma_{33}$ (see text), is also illustrated in Fig. 3 *d*.

would be some average between the $P_1$ and $P_2$ lineshapes. Obviously this is not the case, because $P_1$ and $P_2$ are practically the same, whereas $S_+$ differs from $P_1$ and $P_2$ significantly (Fig. 2). It will be shown below, that $T_{2e}$ anisotropy provides an explanation for the observed lineshape in the diagonal spectrum. Less pronounced than the difference between $S_+$ and $P_2$, but still well visible, is the lineshape change in $S_+$ as a function of $t_m$ (Fig. 4). Especially for TMV, the spectral intensity around the $\sigma_{22}$ chemical shift position is observed to shrink with respect to the lineshape as a whole at increasing $t_m$. Below, this effect will be tentatively assigned to anisotropic spin diffusion.

## DISCUSSION

As demonstrated previously, a combination of slow overall motion of the rod-shaped viruses M13 and TMV about their viral axis and fast restricted backbone motion of the encapsulated nucleic acid molecule can provide a consistent explanation for the motional effects on the observed $^{31}P$ NMR powder lineshapes and transversal relaxation (Magusin and Hemminga, 1993b, 1994). We have employed 2D $^{31}P$ exchange NMR spectroscopy to investigate the slow overall rotation of the rod-shaped virions about their length axis in more detail. The absence of off-diagonal broadening in exchange spectra recorded for TMV with mixing times $t_m \leq 1$ s immediately shows that the diffusion coefficient $D_o$ for overall motion of 30% TMV is below the upper limiting value of 3 Hz, which we have previously estimated from nonspinning transversal relaxation assuming it to be caused by slow overall motion only (Magusin and Hemminga, 1993b). MAS $T_{2e}$ studies have revealed the presence of an additional relaxation mechanism, perhaps related to fast backbone motions of the encapsulated RNA molecule (Magusin and Hemminga, 1994), which could well be responsible for half of the observed nonspinning relaxation. Because $T_{2e} \propto D_o^{-1/3}$ (see definition below Eq. 4), this would indicate that $D_o$ is actually in the order of $10^{-1}$ Hz. Indeed, slow overall rotation in the sub-Hz range would be consistent with the absence of broadening in exchange spectra recorded with $t_m = 1$ s. In contrast to TMV, the exchange spectra obtained for M13 already start to broaden for $t_m = 0.01$ s, which roughly agrees with the 50 Hz estimated for overall motion from nonspinning relaxation.

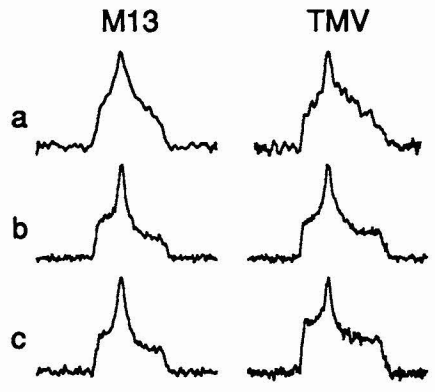


FIGURE 4 1D spectra (*a*) and diagonal spectra for $t_m = 0.01$ s (*b*) and 1 s (*c*) for M13 and TMV, respectively.

To extract quantitative information from the experimental results obtained for M13, the previous model for nonspinning samples (Magusin and Hemminga, 1993a) has been extrapolated to 2D exchange NMR experiments. In both the previous and present models, the motions of the nucleic acid phosphodiesters are collectively described as fast, restricted rotation about the virion length axis characterized by a single "cumulative amplitude" $\lambda$, which may be compared to the general order parameter $S$ in model-free relaxation analyses (Lipari and Szabo, 1982a, 1982b). Of course, uniaxial rotation about the viral axis is a simplified model to describe the net effects of the various types of constrained and concerted backbone motions that occur inside M13 or TMV. The cumulative amplitude $\lambda$ may be regarded as a parameter characterizing the pseudo-static motional narrowing of 1- and 2D $^{31}P$ powder lineshapes caused by fast backbone motions. In the analysis of the 2D exchange spectra presented in this paper, $\lambda$ is not treated as a variable fitting parameter, but is fixed to the value previously estimated on the basis of the observed 1D lineshape (Magusin and Hemminga, 1993b). Another simplification is that our model distinguishes between overall diffusion of the virus particles during the mixing time $t_m$, and virion diffusion during the evolution time $t_1$ and acquisition time $t_2$. As mentioned under Theory, this artificial distinction speeds up the spectral analysis, because various 2D exchange spectra can be simulated using a single set of subspectra generated for an *a priori* selected value for the overall diffusion coefficient $D_o$ during $t_1$ and $t_2$. $D_o$ has already been determined independently on the basis of $T_{2e}$ measurements (Magusin and Hemminga, 1993b). *A posteriori*, $D_o$ and the overall diffusion coefficient extracted from off-diagonal broadening during $t_m$ will be compared. Despite its relatively simple character, our model still contains quite a number of parameters. In our analysis of 2D exchange spectra, however, $\lambda$, $D_o$, and the chemical shift tensor values $\sigma_{11}$, $\sigma_{22}$ and $\sigma_{33}$ are treated as constants with values based on previous lineshape and relaxation analysis. As will be discussed, the change of the 2D exchange spectrum at varying $t_m$ will be solely interpreted in terms of slow overall rotation of the virus particles about their length axis during $t_m$, which for homogeneous diffusion is characterized by the coefficient $D$ as a single fitting parameter only, and for inhomogeneous diffusion by the central diffusion coefficient $D_c$ and the distribution width $W$.

We have used Eqs. 9 and 10 to calculate 16 subspectra $I_n^{\pm}(\omega_1, \omega_2 | \Delta\Omega'_n)$, where $\Delta\Omega'_n = (0, \Delta\Psi_n, 0)$, $\Delta\Psi_n$ being equidistant multiples of 0.2 rad between 0.0 and 3.0 rad. For the restriction half angle $\lambda$ and the overall diffusion coefficient $D_o$, the values 0.75 rad and 50 Hz were first selected in accordance with the outcome from previous analyses of 1D $^{31}P$ lineshapes and transversal relaxation (Magusin and Hemminga, 1993b). Using this set of subspectra and assuming a gaussian distribution of rotation angles $\Delta\Omega'_n$ typical for

homogeneous, uniaxial diffusion (Eq. 6), subspectra combinations according to Eq. 8 can be made that fit well to every experimental exchange spectrum recorded for M13 separately. Spectra recorded for mixing times $t_m$ = 0.01, 0.1 and 1 s are best simulated for different diffusion coefficients $D$ = 15, 5, and 1.7 Hz, respectively (Fig. 5). However, no $D$ value is found that produces good fits to the three spectra together. In a first attempt, we tried to reduce the difference among the resulting $D$ values by introducing extra transversal relaxation during $t_1$ and $t_2$ into the model. This adds an extra $t_m$-independent spectral broadening to simulations, which especially influences the simulated spectra for short mixing times. If, for instance, subspectra are generated for $D_o$ = 400 Hz instead of $D_o$ = 50 Hz, the $t_m$-independent homogeneous broadening is roughly doubled (see definition of $T_{2e}$ below Eq. 4). As a result, reduced $D$ values of 6.9, 3.6, and 1.3 Hz are obtained for $t_m$ = 0.01, 0.1, and 1 s, respectively. Indeed, increasing $D_o$ reduces the $D$ value resulting from spectral simulation for short $t_m$ more than for long $t_m$ and thereby suppresses the difference among $D$ values found for different $t_m$. However, $D_o \geq$ 400 Hz would be inconsistent with the diffusion coefficient of 50 Hz found in our previous relaxation analysis (Magusin and Hemminga, 1993b) and would also disagree with the extremely narrow diagonal ridge observed in the exchange spectrum recorded for $t_m$ = 10 $\mu$s (not shown).

Obviously, the simple model employed to analyze 2D exchange spectra in the above discussion cannot provide a consistent explanation for the exchange spectra recorded at various mixing times together. To remove this inconsistency, we have tested several model variants on the basis of some previously expressed, tentative ideas (Magusin and Hemminga, 1993b). For instance, because simulations of the 1D $^{31}$P NMR spectrum of 30% M13 are slightly improved by the assumption that the backbone of M13 DNA consists of 83% immobile and 17% mobile phosphodiesters, we have tried both fast- and intermediate-exchange two-component models. Under fast-exchange conditions, on the one hand, motional narrowing would cause the contribution by a mobile phosphodiester fraction to the 2D exchange spectrum to be a narrow intensity pattern close to the diagonal even at long $t_m$. Such effect could qualitatively explain why the diagonal ridge observed in M13 spectra recorded with $t_m$ = 1 s is relatively narrow, as compared with the already quite broad diagonal ridge observed for $t_m$ = 0.01 s. In the intermediate exchange case, on the other hand, the mobile phosphodiesters undergoing motions in the $10^4$-$10^5$ Hz frequency range would contribute a broad, practically $t_m$-invariant intensity pattern to the exchange spectrum recorded with $t_m \geq 10^{-2}$ s. A broad intensity pattern in the exchange spectrum would lead to an overestimation of the overall diffusion coefficient $D$, especially at short $t_m \approx 10^{-2}$ s. This could possibly explain the difference between the estimated $D$ values at various $t_m$. We have also checked whether 2D exchange spectra of M13 actually reflect some preferential orientation of the phosphodiesters with respect to the viral axis. An anisotropic distribution of phosphodiester orientations, e.g., such that most $\sigma_{33}$ components were parallel to the viral axis, could lead to a narrower intensity pattern at long $t_m$ than expected from a random distribution. On the basis of a previous comparison of structural parameters (Magusin and Hemminga, 1993b), a model has been set up in which 83% phosphodiesters are oriented with respect to the viral axis as in B-DNA with respect to the helical axis. Unfortunately, none of the above three model variants is able to remove the apparent inconsistency between the exchange spectra recorded with various $t_m$, or even to produce better simulations for each of the experimental spectra separately. Our previous, tentative assumption that two phosphodiester fractions exist within M13, can neither be justified nor rejected on the basis of the M13 exchange spectra.

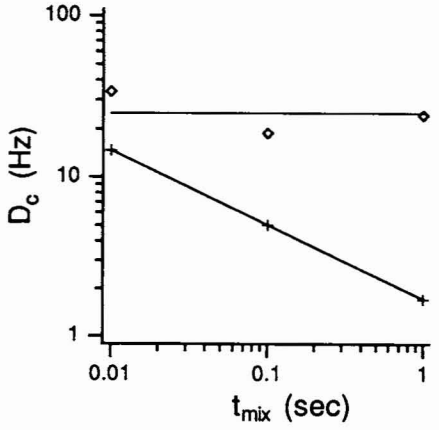


FIGURE 5 Plot of the (central) overall diffusion coefficient estimated from exchange spectra of M13 against $t_m$. (+) Homogeneous diffusion; (◇) a log-gaussian distribution of diffusion coefficients with $W$ = 1.5 (Eq. 11).

As noted previously (Magusin and Hemminga, 1993b), $^{31}$P transversal relaxation decays observed for M13 are steeper at short echo times $2\tau < 0.2$ ms, than the theoretical curves that fit best to the whole set of echoes measured up to $2\tau$ = 1.6 ms (Fig. 6). This could indicate that some of the virions diffuse more rapidly than expected from the average diffusion coefficient. Such motional inhomogeneity would be characterized by a spread of overall diffusion coefficients. Assuming a log-gaussian distribution characterized by a central value $D_c$ and a width parameter $W$ (Wefing et al., 1988), the spread of rotation angles $P'(\Delta\Omega' \mid t_m)$ resulting from the overall diffusion of the rod-shaped virions about their length axis can be derived as a function of $t_m$ (Eq. 11). Using the same sets of subspectra $I_n^{\pm}(\omega_1, \omega_2 \mid \Delta\Omega'_n)$ as employed for testing the models discussed above, combinations can be made for different values for $D_c$ and $W$ and compared with the experimental spectra. For each of the above discussed models adapted for motional inhomogeneity, a pair of values for $D_c$ and $W$ can be obtained that consistently explain the observed M13 spectra recorded with $t_m$ = 0.01, 0.1, and 1 s. For instance, using the single component model with $D_o$ = 50 Hz and $\lambda$ = 0.75 rad, exchange spectra can be simulated for $D_c$ = 25 Hz and $W$ = 1.5, which fit well to the three experimental spectra (Figs. 5 and 7). Most virions in 30% M13 gels thus seem to undergo overall rotational diffusion

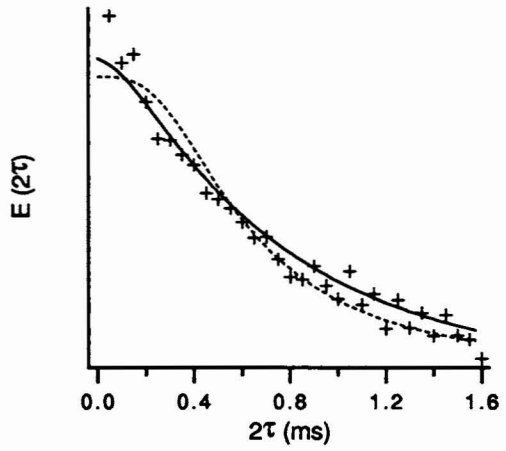


FIGURE 6 Simulation of nonspinning transversal relaxation for a log-gaussian distribution of diffusion coefficients with $D_c$ = 25 Hz and $W$ = 1.5 (Eq. 11), superimposed on 3-ms exponential relaxation caused by fast nucleic acid backbone motions, as estimated from MAS experiments (see text). The broken line illustrates the previously published simulation for homogeneous overall motion with a diffusion coefficient of 50 Hz (Magusin and Hemminga, 1993b).

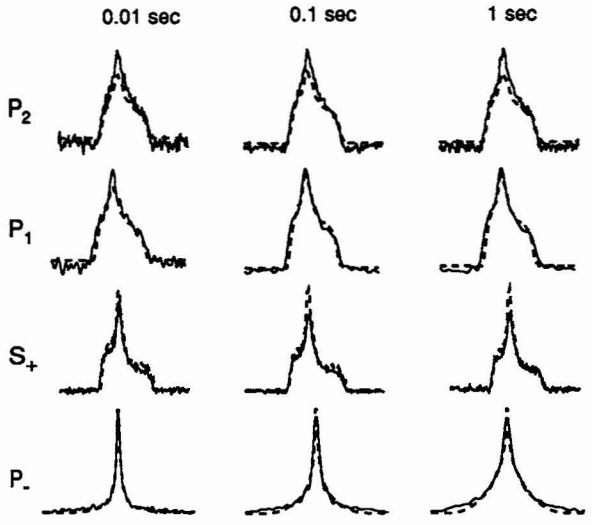


FIGURE 7 Comparison of theoretical (solid line) and experimental (dashed line) 2D exchange spectra of M13 for various $t_m$ values reflected by projection and diagonal spectra (see Fig. 2). Theoretical spectra have been calculated for a distribution of diffusion coefficients with $D_c$ = 25 Hz and $W$ = 1.5 (Eq. 11) and fitted to the experimental 2D exchange spectra as a whole.

with coefficients in a range of three decades around 25 Hz, i.e., between 1 and 1000 Hz. An upper limit of 1000 Hz would still agree with the absence of sideband broadening in the observed MAS spectra (Magusin and Hemminga, 1994). The central overall diffusion coefficient $D_c$ = 25 Hz estimated from the exchange spectra is twice as small as the homogeneous overall diffusion coefficient $D_0$ = 50 Hz determined from transversal relaxation. Because $T_{2e}$ is inversely proportional to the cube root of the diffusion coefficient, slow overall diffusion seems to be responsible for about $2^{-1/3}$ = 80% of the observed relaxation. The remaining 20% is indicative for some extra relaxation mechanism with $T_{2e} \approx 3$ ms at a $^{31}$P resonance frequency of 121.5 MHz. Such value would well agree with the MAS $T_{2e}$ value of 1.3 ms previously measured at 202.5 MHz for 25% M13, which we ascribed to fast nucleic acid backbone motions (Magusin and Hemminga, 1994). Indeed, if we repeat the previous simulation of the nonspinning transversal relaxation decay while this time taking into account a log-gaussian distribution with $W$ = 1.5 around $D$ = 25 Hz and extra relaxation with $T_2 \approx$ 3 ms by fast backbone motions, an even better fit is obtained than the previously published simulation (Fig. 6) (Magusin and Hemminga, 1993b). Motional inhomogeneity in gels of M13 is probably caused by the tendency of the bacteriophages to form variously sized aggregates (Day et al., 1988).

The agreement between exchange spectra simulated for $D_c$ = 25 Hz and $W$ = 1.5 and the experimental M13 spectra recorded with various $t_m$ is illustrated by the theoretical and experimental $P_1$ projections, $P_-$ projections and $S_+$ sections in Fig. 7. $P_2$ projections of the experimental spectra are slightly larger than those of the simulated spectra that fit best to the observed 2D spectra as a whole. This could be an experimental artifact caused by the merging of the first two $^{31}$P pulses in the pulse sequence for $t_1$ = 0 (Fig. 1). The good fit between experimental and simulated spectra indicates that the difference between the projection spectra and the diagonal spectrum observed for M13 and TMV can mainly be explained by the anisotropy of the transversal relaxation caused by slow overall rotation. $T_{2e}$ anisotropy could perhaps also explain the fact that the $^{31}$P NMR lineshape of 10% TMV (Cross et al., 1983) seems to be less motionally narrowed than the one observed for 30% TMV observed by us.

The relative shrinking of the $\sigma_{22}$ discontinuity on the diagonal in 2D exchange spectra of M13 and TMV with respect to the other two discontinuities for $t_m > 0.01$ s, is not well accounted for by our model. We tend to assign this effect to $^{31}$P spin diffusion. Distances between neighboring phosphodiesters in M13 are probably similar to those in TMV, which vary between 5.4 and 7.5 Å (Opella and DiVerdi, 1982; Stubbs and Stauffacher, 1981). Such internuclear distances indicate weak $^{31}$P-$^{31}$P couplings of $\leq$100 Hz. Spin diffusion effects would thus indeed be expected in exchange spectra for $t_m > 0.01$ s. Effective homonuclear coherence transfer, however, would be limited to neighboring $^{31}$P nuclei with chemical shifts that differ less than the coupling size, thus 1 ppm at 121.5 MHz, unless motions in the $10^3$-$10^4$-Hz range would be present, bridging chemical shift differences across the $^{31}$P powder resonance line. A narrow shift-matching condition would be consistent with the narrow ridge observed in exchange spectra of TMV. The shrinking of the $\sigma_{22}$ discontinuity is most easily explained in a qualitative manner by the use of our M13 model in which the shift tensor orientations of neighboring $^{31}$P nuclei are assumed to be completely uncorrelated. As illustrated by the powder lineshape itself with its maximum at $\sigma_{22}$, any $^{31}$P spin within M13 would have relatively many $^{31}$P spins with a chemical shift close to $\sigma_{22}$ around itself. Because the effectiveness of spin diffusion between $^{31}$P spins depends on their chemical

shift difference, $^{31}$P spins with a chemical shift close to $\sigma_{22}$ relax faster than other spins. This would explain the observed shrinking of the $\sigma_{22}$ discontinuity on the diagonal in exchange spectra of M13. For TMV, a similar explanation would have to include the regular geometry of the encapsulated RNA molecule, which causes the chemical shift tensors of neighboring phosphodiesters not to be randomly oriented with respect to each other. Because motions in the $10^3$-$10^4$-Hz range seem to be largely absent in concentrated M13 gels (Magusin and Hemminga, 1994), spin diffusion effects in exchange spectra of M13 are probably concentrated on the diagonal, like for TMV. Therefore, the various observed off-diagonal intensity patterns probably reflect the pure effect of slow overall motion of the rod-shaped viruses only.

## CONCLUSION

2D exchange $^{31}$P NMR spectroscopy is a powerful technique for studying the slow overall motion of the rod-shaped viruses M13 and TMV. Spectra of 30% TMV recorded with $t_m \leq 1$ s do not show any off-diagonal broadening, indicating that TMV particles in concentrated gels are extremely immobile even at a time scale of seconds. For 30% M13, a log-gaussian distribution around 25 Hz of rotational diffusion coefficients mainly spread between 1 and $10^3$ Hz must be introduced to reproduce the 2D exchange NMR spectra recorded at various mixing times in a consistent way. Taking this distribution and a minor relaxation contribution caused by fast backbone motion into account, an even better fit to the nonspinning transversal relaxation decay is obtained than published previously for homogeneous diffusion (Magusin and Hemminga, 1993b). The shrinking of the $\sigma_{22}$ discontinuity on the diagonal with respect to the lineshape as a whole at $t_m \geq 0.1$ s cannot be explained by slow overall motion, but seems to be caused by spin diffusion between $^{31}$P nuclei with chemical shifts that differ by <1 ppm.

This paper is the last one in a series of four in which models have been developed and tested to explain the results of various $^{31}$P NMR experiments observed for intact M13 and TMV virus particles in concentrated gels. At this stage, it is worthwhile to present a brief overview to show advantages and limitations of the specific NMR techniques employed by us for investigating large nucleoprotein complexes such as M13 and TMV in general (Table 1). In these systems, $^{31}$P nuclei represent natural NMR labels for studying structural and dynamic properties of the nucleic acid backbone selectively, even when the complex mainly consists of proteins. High-power $^1$H-decoupled 1D $^{31}$P NMR spectra observed for nonspinning samples of these complexes contain a single broad resonance line reflecting the average $^{31}$P CSA typical for phosphodiesters in DNA or RNA. The strong CSA broadening, however, tends to mask the small differences among the phosphodiesters of the complexed nucleic acid (Magusin and Hemminga, 1993b). Such phosphodiester inhomogeneity, indicating, e.g., inequivalence among binding sites, is best studied using $^{31}$P MAS NMR spectroscopy (Magusin and Hemminga, 1994). $^{31}$P MAS NMR spectra of TMV show two resolved sideband patterns with an overall intensity ratio of ~2, reflecting the three types of phosphodiesters in TMV. In contrast, MAS NMR spectra of M13 only contain a single, relatively broad centerband flanked by sidebands, indicating that a continuous distribution of phosphodiester conformations exists within the phage. Nucleic acid backbone motions perhaps underlie the observed decrease of inhomogeneous linewidth at increasing temperature and hydration by partly averaging the conformational differences.

$^{31}$P NMR spectroscopy is also a powerful tool to study the mobility of the complexed nucleic acid in a broad frequency range. For the viruses M13 and TMV studied by us, the observed motional narrowing of the $^{31}$P NMR lineshapes is indicative for restricted motion with frequencies in the order of the static linewidth or larger ($\geq 10^4$ Hz). In contrast, $^{31}$P transversal relaxation measured for nonspinning M13 at various temperatures and hydration percentages indicates motion in the slow or intermediate frequency region. We have shown by simulation that simple models, such as isotropic and rigid-rod diffusion, cannot reproduce the experimental data. Instead, a consistent description is offered by a combined diffusion model in which the lineshape is dominated by fast

**TABLE 1 Types of information about phosphodiester structure, nucleic acid backbone motion, and overall virion motion obtained in our study of M13 and TMV illustrating the use of different $^{31}$P NMR techniques for investigating nucleoprotein complexes, in general**

| Type of spectroscopy | Object ofanalysis | Phosphodiesterstructure | Nucleic acid backbone motion | Virion overall motion |
|---|---|---|---|---|
| Nonspinning 1D $^{31}$P NMR | Lineshape | Average conformation | Cumulative amplitude | |
| | Transversal relaxation | | | Average diffusion coefficient |
| MAS 1D $^{31}$P NMR | Centerband lineshape | Distribution of conformations | Conformational fluctuation | |
| | Sideband intensities | | Cumulative amplitude | |
| | Transversal relaxation | | Effective frequency | Average diffusion coefficient |
| Nonspinning 2D exchange $^{31}$P NMR | Lineshape analysis | | | Distribution of diffusion coefficients |

For the rod-shaped M13 and TMV viruses, the observed motional effects on $^{31}$P NMR spectra and transversal relaxation can be explained by a combination of slow rotational diffusion of the virions about their length axis and fast restricted motions of the encapsulated nucleic acid molecules. In contrast to the three distinct types of phosphodiesters in TMV, a continuous distribution of phosphodiester conformations seems to exist in M13.

internal DNA motions and transversal relaxation reflects slow overall rotation of the virions about their length axis. The presence of phosphodiester motions with frequencies $\geq 10^5$ Hz is confirmed by the fact that sideband intensities in MAS spectra of dilute M13 gels seem to be affected by motions without the sidebands being broadened (Magusin and Hemminga, 1994). The presence of slow motion is confirmed by the fact that $^{31}$P transversal relaxation is strongly suppressed by MAS. From the spinning rate-dependent part of transversal relaxation, overall diffusion coefficients can be extracted in perfect agreement with those obtained from transversal relaxation under nonspinning conditions. The part of transversal relaxation that does not depend on the spinning rate is assigned to the same phosphodiester motions that also cause the motional narrowing of the $^{31}$P resonance line.

If the nucleic acid backbone is sufficiently immobilized within a nucleoprotein complex, detailed information about motion of the complex in the sub-kHz range can be obtained by use of 2D exchange $^{31}$P NMR spectroscopy. Comparison of the off-diagonal intensity patterns in 2D exchange spectra recorded with various mixing times provides insight in the distribution of motional amplitudes and correlation times involved. 2D exchange spectra of TMV demonstrate that the virus is less mobile than estimated from transversal relaxation alone (see Discussion section), indicating that overall motion causes only part of the observed nonspinning $T_{2e}$ relaxation. Exchange spectra of M13 obtained for various mixing times suggest that overall diffusion of the virus particles in the sticky gels is inhomogeneous.

We are grateful to Ruud Spruijt for isolation of M13 and TMV, Jan Jaap ter Horst for experimental assistance, and Klaus Schmidt-Rohr and Arno Kentgens for helpful discussions. This research was supported by the Netherlands Foundation of Biophysics with the financial support of the Netherlands Organization for Scientific Research (NWO).

## REFERENCES

Cross, T. A., S. J. Opella, G. Stubbs, and D. L. D. Caspar. 1983. Phosphorus-31 nuclear magnetic resonance of the RNA in tobacco mosaic virus. *J. Mol. Biol.* 170:1037–1043.

Day, L. A., C. J. Marzec, S. A. Reisberg, and A. Casadevall. 1988. DNA packing in filamentous bacteriophages. *Annu. Rev. Biophys. Chem.* 17: 509–539.

Edmonds, A. R. 1960. Angular Momentum in Quantum Mechanics. Princeton University Press. Princeton, New Jersey. 146 pp.

Fenske, D. B., and H. C. Jarrell. 1991. Phosphorus-31 two-dimensional solid-state exchange NMR. Application to model membrane and biological systems. *Biophys. J.* 59:55–69.

Haeberlen, U. 1976. High Resolution NMR in Solids: Selective Averaging. Academic Press, New York.

Herzfeld, J., and A. E. Berger. 1980. Sideband intensities in NMR spectra of samples spinning at the magic angle. *J. Chem. Phys.* 73:6021–6030.

Kimich, R., and E. Fischer. 1994. One- and two-dimensional pulse sequences for diffusion experiments in the fringe field of superconducting magnets. *J. Magn. Res. Ser. A.* 106:229–235.

Lipari, G., and A. Szabo. 1982a. Model-free approach to the interpretation of nuclear magnetic resonance relaxation in macromolecules. 1. Theory and range of validity. *J. Am. Chem. Soc.* 104:4546–4559.

Lipari, G., and A. Szabo. 1982b. Model-free approach to the interpretation of nuclear magnetic resonance relaxation in macromolecules. 2. Analysis of experimental results. *J. Am. Chem. Soc.* 104:4559–4570.

Magusin, P. C. M. M., and M. A. Hemminga. 1993a. A theoretical study of rotational diffusion models for rod-shaped viruses: the influence of motion on $^{31}$P NMR lineshapes and transversal relaxation. *Biophys. J.* 64:1851–1860.

Magusin, P. C. M. M., and M. A. Hemminga. 1993b. Analysis of $^{31}$P NMR lineshapes and transversal relaxation of bacteriophage M13 and tobacco mosaic virus. *Biophys. J.* 64:1861–1868.

Magusin, P. C. M. M., and M. A. Hemminga. 1994. Analysis of $^{31}$P MAS NMR lineshapes and transversal relaxation of bacteriophage M13 and tobacco mosaic virus. *Biophys. J.* 66:1197–1208.

Marion, D., and K. Wüthrich. 1983. Application of phase sensitive two-dimensional correlated spectroscopy (COSY) for measurements of proton-proton spin-spin coupling constants in proteins. *Biochem. Biophys. Res. Commun.* 113:967–974.

Opella, S. J., and J. A. DiVerdi. 1982. Properties of the phosphodiester backbone of duplex DNA and filamentous bacteriophage DNA. *In* Biochemical Structure Determination by NMR. A. A. Bothner-By, J. Glickson, and B. D. Sykes, editors. Marcel Dekker, New York. 149–168.

Schmidt-Rohr, K., and H. W. Spiess. 1991. Nature of nonexponential loss of correlation above the glass transition investigated by multidimensional NMR. *Phys. Rev. Lett.* 66:3020–3023.

Slichter, C. P. 1978. Principles of Magnetic Resonance. Springer-Verlag, Berlin.

Stubbs, G., and C. Stauffacher. 1981. Structure of the RNA in tobacco mosaic virus. *J. Mol. Biol.* 152:387–396.

Tomasselli, M., B. H. Meier, P. Robyr, U. W. Suter, and R. R. Ernst. 1993. Direct measurement of xenon exchange between gas and liquid phase by 2D NMR. *Chem. Phys. Lett.* 214:1–4.

Wefing, S., S. Kaufmann, and H. W. Spiess. 1988. Two-dimensional exchange NMR of powder samples. II. The dynamic evolution of two-time distribution functions. *J. Chem. Phys.* 89:1234–1244.

Wefing, S., and H. W. Spiess. 1988. Two-dimensional exchange NMR of powder samples. I. Two-time distribution functions. *J. Chem. Phys.* 89: 1219–1233.